

Rapid Communications

Rapid Communications are intended for the accelerated publication of important new results and are therefore given priority treatment both in the editorial office and in production. A Rapid Communication in Physical Review B should be no longer than four printed pages and must be accompanied by an abstract. Page proofs are sent to authors.

Evidence for quantum states corresponding to families of stable and chaotic classical orbits in a wide potential well

T. M. Fromhold, A. Fogarty, L. Eaves, F. W. Sheard, M. Henini, T. J. Foster, and P. C. Main
Department of Physics, University of Nottingham, Nottingham NG7 2RD, United Kingdom

G. Hill

Department of Electronic and Electrical Engineering, University of Sheffield, Mappin Street, Sheffield S1 3JD, United Kingdom
 (Received 12 January 1995; revised manuscript received 13 March 1995)

The quantized energy-level spectrum corresponding to stable and chaotic classical electron motion in a wide 60-nm potential well with a strong tilted magnetic field is studied by magnetotunneling spectroscopy. At low bias voltages ($V \leq 1$ V) and for tilt angles θ of the magnetic field within the domain of hard classical chaos, the current-voltage characteristic $I(V)$ reveals several distinct series of resonances which evolve rapidly with V and θ . In this regime, a hierarchy of unstable but periodic orbits is identified and related to fluctuations in the density of levels in the well and to the observed magnetotunneling characteristics. Widely spaced resonances in $I(V)$ observed for $V \geq 1$ V originate from the appearance of stable orbits in regions of the classical phase space accessible to the tunneling electrons.

During the past three years several experiments have investigated the influence of chaos on quantum transport in mesoscopic condensed-matter systems.¹⁻³ In a recent publication we have demonstrated the close relation between unstable periodic orbits and the tunneling characteristics of a GaAs/(AlGa)As resonant tunneling diode (RTD) containing a 120-nm-wide potential well with a strong tilted magnetic field B .³ Electrons in the potential well exhibit strongly chaotic classical motion for a range of tilt angles θ relative to the normal to the well walls. In this regime, the current-voltage characteristics $I(V)$ reveal two distinct series of periodic resonances which change dramatically with both θ and the applied bias voltage.³ The resonant peaks originate from periodic variations in the density of levels in the well that can be related to unstable closed classical orbits by the well-known trace formula.^{3,4} In these orbits the electron makes one or two successive collisions on the collector barrier for each hit on the emitter barrier. Resonant features associated with more complex trajectories are not resolved for the 120-nm-wide well because the electrons cannot complete the orbits before emitting a longitudinal optic (LO) phonon.

In this paper we report an investigation of a GaAs/(AlGa)As RTD in which the potential well is sufficiently narrow (60 nm) for the electrons to complete several periodic orbits of more complex shape than those identified for the 120-nm-wide well described in our earlier papers.³ They involve multiple bounces on the confining barriers before emission of an LO phonon. For bias voltages $V \leq 1$ V, the classical motion exhibits predominantly strong chaos and the $I(V)$ characteristics contain several series of resonances

which evolve rapidly with θ and V . We relate the resonances to a hierarchy of unstable periodic classical orbits in the well. At higher bias, stable orbits become accessible to the tunneling electrons. The onset of orbital stability is characterized by a changeover to widely spaced oscillations in the $I(V)$ plots. In our earlier studies³ the electric field in the 120-nm-wide well was insufficient to explore this domain of soft classical chaos.

The conduction-band profile of the RTD is shown in Fig. 1. Details of the sample composition are given elsewhere.⁵ Current flows as electrons tunnel from the two-dimensional

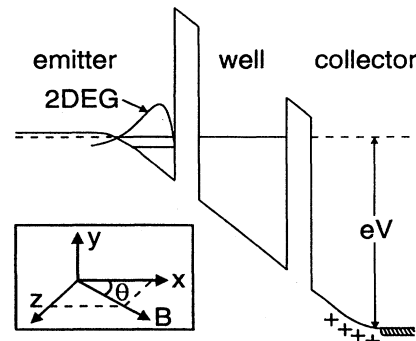


FIG. 1. Schematic conduction-band profile of the RTD under bias voltage V showing the 2DEG in the emitter contact. Inset: tilt angle θ of magnetic field B relative to the tunneling (x) direction.

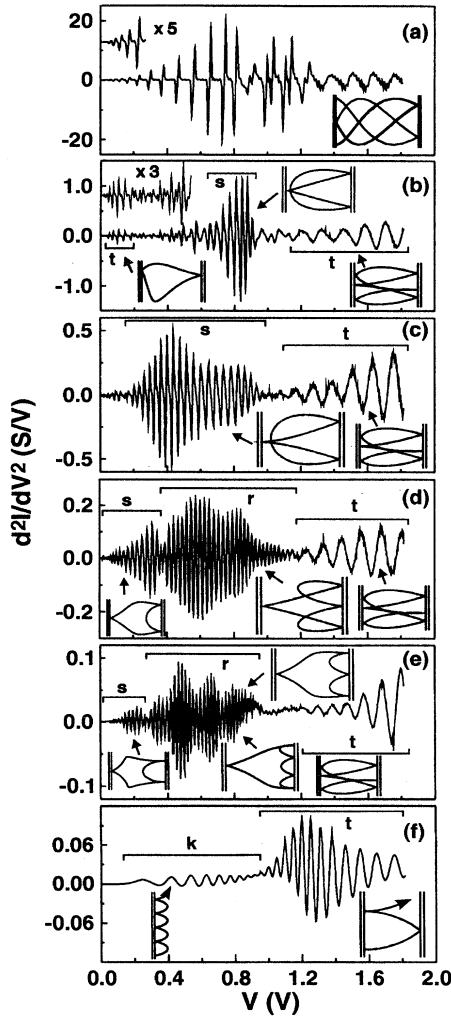


FIG. 2. d^2I/dV^2 vs V plots for the RTD with $B=10$ T and $\theta=$ (a) 0° , (b) 20° , (c) 30° , (d) 40° , (e) 50° , (f) 90° . The t , s , and r resonances observed for $V \leq 1$ V are related to type-1, -2, -3, and -4 unstable periodic orbits inset projected on the x - y plane. The widely spaced t resonances seen for $V \geq 1$ V are associated with stable traversing orbits (right insets).

electron gas (2DEG) in an undoped spacer layer adjacent to the doped emitter contact into the many quantized energy levels in the wide 60-nm well, and then from the well into the collector contact. The tunneling characteristics are shown in Fig. 2 for a range of tilt angles with $B=10$ T. When $\theta=0^\circ$, a single series of weak periodic oscillations is observed in $I(V)$, and more clearly in the d^2I/dV^2 versus V plots [Fig. 2(a)]. These resonances have a voltage period $\Delta V \approx 50$ mV and originate from resonant tunneling into the electric subbands of the well.⁵

As the magnetic field is tilted, the resonant structure becomes more complicated. When $\theta=20^\circ$, a single series of resonances is observed for $V \leq 200$ mV, labeled t in Fig. 2(b). These t resonances evolve smoothly from the oscillatory structure observed at similar bias voltages when $\theta=0^\circ$. A Fourier transform of the data for voltages in the range $200 \leq V \leq 600$ mV shows that two different sets of quasiperi-

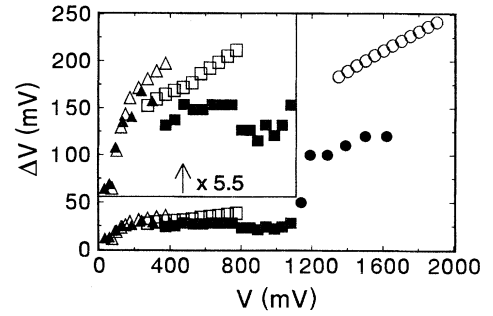


FIG. 3. Variation of voltage spacing ΔV with V for experimental s series (full triangles), r series (full squares), and t series (full circles) observed for $\theta=40^\circ$ ($B=10$ T) and theoretical values based on periods of unstable type-2 orbits (open triangles), unstable type-3 orbits (open squares), and stable traversing orbits (open circles), respectively. ΔV values for data in top LH box increased by factor 5.5.

odic oscillations coexist. However, only one series [labeled s in Fig. 2(b)] with $\Delta V \approx 40$ mV is observed for $600 \leq V \leq 1000$ mV. At higher V new features, t resonances, appear with a large voltage period $\Delta V \approx 100$ mV. Similar oscillations are observed at high voltages for all values of θ . At $\theta=30^\circ$ the s and t series are observed for distinct voltage ranges shown by the brackets in Fig. 2(c). These voltage ranges change as θ is increased beyond 30° . When $\theta=40^\circ$, the s and t resonances are separated by a third series of oscillations observed for voltages in the range $375 \leq V \leq 1200$ mV [Fig. 2(d)]. For these resonances, referred to as the r series, $\Delta V \approx 25$ mV. The variation of ΔV with V is shown for the r , s , and t oscillations at $\theta=40^\circ$ in Fig. 3. A weak low-frequency modulation of the amplitudes of the r resonances can be seen in Fig. 2(d). This modulation is stronger at $\theta=50^\circ$ [Fig. 2(e)]. For $\theta \geq 65^\circ$, the s and r series are replaced by new low-frequency oscillations which evolve into the two sets of resonances observed at $\theta=90^\circ$ [labeled k and t in Fig. 2(f)].

In a classical picture, the electron orbits in the well are regular when $\theta=0^\circ$ or 90° , corresponding to either traversing orbits which intersect with the two barriers in turn [Fig. 2(a) inset and Fig. 2(f) right inset] or skipping orbits along the left-hand (LH) barrier [Fig. 2(f) left inset].^{5,6} For these angles the correspondence principle relates the energy-level spacing $\Delta E = h/\tau$ to the classical time τ between successive collisions on the LH barrier.⁶ This level spacing determines the voltage spacing of resonances in the d^2I/dV^2 versus V plots.⁶ When $\theta=0^\circ$, and for $\theta=90^\circ$ when $V > 950$ mV, there are traversing orbits which produce the t resonances in Figs. 2(a) and 2(f). At $\theta=90^\circ$, skipping orbits on the LH barrier exist for $V < 950$ mV, and produce the k resonances in Fig. 2(f).^{5,6}

Although the classical motion in the well exhibits predominantly strong chaos for θ in the range $15^\circ \leq \theta \leq 75^\circ$ with $V \leq 1$ V, many unstable but periodic orbits exist. As shown by Gutzwiller,⁴ each unstable closed orbit produces periodic clustering of the quantized energy levels with an energy period $\Delta E_p = h/T_p$, where T_p is the orbital period for given V .^{3,4} This clustering creates regular fluctuations in the density of levels which modulate the tunneling rates from the

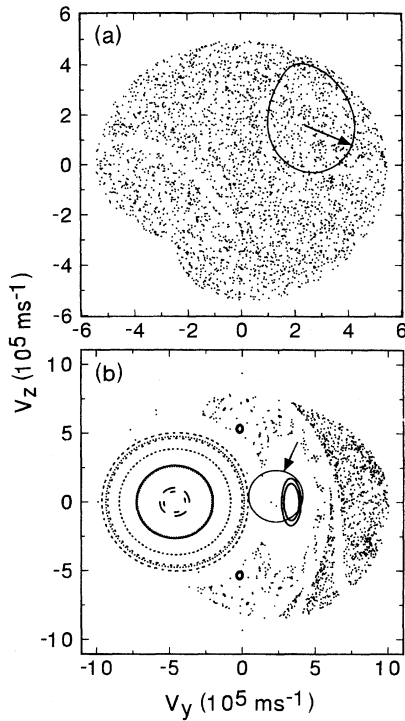


FIG. 4. Poincaré sections showing (v_y, v_z) for 3400 collisions with the LH barrier generated from 17 different starting velocities consistent with the electron injection energy at $B=10$ T, $\theta=40^\circ$, and $V=300$ mV (a), and 1900 mV (b). Solid curves (arrowed): range of lateral velocity components for electrons entering the well from the 2DEG.

2DEG into the well, thereby giving rise to periodic oscillations in the $I(V)$ plots.^{3,7} The voltage spacings of the resonances are related to the periods T_P by $\Delta V = Lh/e\langle x \rangle T_P$, where for given V the effective electrical width L of the RTD (Ref. 3) is obtained by solving Poisson's equation throughout the device using a one-parameter variational wave function to model the emitter bound state,³ and the mean distance $\langle x \rangle$ between the 2DEG and the electron in the well is calculated for each type of orbit. To analyze the resonant structure observed in the $I(V)$ plots we have searched for periodic classical orbits in the well accessible to the tunneling electrons. We require that the periods T_P are sufficiently short (<0.6 ps) that the spacing ΔE_P of the level clusters exceeds the broadening produced by LO phonon emission. This ensures that the associated resonances can be resolved in our tunneling spectra. The numerical techniques used to locate the periodic orbits are described in Ref. 3.

For $V \leq 1$ V the classical motion of electrons injected into the well is strongly chaotic. This can be seen from the Poincaré sections⁴ for the system, which are similar to that shown in Fig. 4(a) for $V=300$ mV. The scattered points show the lateral velocity components (v_y, v_z) each time the electron bounces off the LH barrier. The uniform distribution of points demonstrates that the classical motion is strongly chaotic. In this regime, we have identified a hierarchy of distinct unstable periodic orbits involving multiple collisions on the right-hand (RH) barrier, whose properties explain the origin

and θ dependence of the resonances observed for $V \leq 1$ V. These orbits are shown projected onto the x - y plane in the insets to Fig. 2. We refer to an orbit in which the electron makes λ collisions on the RH barrier for each hit on the LH barrier as a type- λ orbit. Calculations of the ranges of V and θ for which each type of orbit exists, together with the ΔV values obtained from the orbital periods, enable us to relate different types of orbit to the distinct series of resonances observed in d^2I/dV^2 .³

In Fig. 2(b), the t resonances indicated by the LH bracket originate from the unstable type-1 orbit (inset left). The s and r series shown in Figs. 2(b), 2(c), 2(d), and 2(e) are associated with unstable type-2 and type-3 orbits, respectively [see, for example, Fig. 2(d) left and center insets]. We attribute the periodic modulation in the amplitudes of the r oscillations observed for $\theta=40^\circ$ and 50° to the coexistence of type-3 and type-4 orbits [Fig. 2(e) upper and central lower insets, respectively]. When $\theta=50^\circ$, these orbits have similar periods (~ 0.35 and ~ 0.40 ps, respectively, when $V=0.8$ V). The two sets of associated fluctuations in the density of levels for the well therefore have similar energy periods. This produces low-frequency beating in the density of levels which modulates the amplitudes of the r resonances.

A quantitative comparison between theory and experiment is now given for $\theta=40^\circ$. We first consider bias voltages $V \leq 1.2$ V corresponding to the domain of unstable accessible orbits. At $\theta=40^\circ$, unstable type-2 and type-3 closed orbits exist for voltages in the ranges $50 \leq V \leq 350$ mV and $200 \leq V \leq 775$ mV, respectively. Figure 3 shows a comparison between ΔV values calculated from the periods of the type-2 and type-3 orbits and measured for the s and r resonances. For both types of orbit, ΔV increases with increasing V as the electrons attain higher speeds in the well. This behavior accords with the V dependence of the ΔV values measured for the s and r resonances. The voltage ranges of the type-2 and type-3 orbits are also in fair agreement with those of the s and r resonances, respectively.

For $V \geq 1.2$ V, the electron orbits in the accessible well are stable for certain initial velocities v_0 at the LH barrier. This can be seen from the Poincaré section calculated for $V=1.9$ V [Fig. 4(b)]. In some regions of the plot the points are distributed uniformly and form a sea of chaos. However, there are also four sets of nested islands (sections through invariant KAM tori⁴) within which (v_y, v_z) lie on families of well-defined curves. When v_0 lies within one of these islands the classical motion is stable. Each set of islands corresponds to a distinct type of stable orbit in which the electron repeats a particular sequence of collisions with the well walls. The solid curve (arrowed) in Fig. 4(b) indicates the range of transverse velocity components of electrons entering the well and is obtained by calculating the classical momentum transferred as the electrons move from the 2DEG to the LH edge of the well.³ This curve intersects with two sets of islands in Fig. 4(b), and so two different types of stable classical orbit are accessible to the tunneling electrons. Orbits within the LH quasicircular islands (for example, the orbit shown in the inset of Fig. 5) intersect with the two confining barriers in turn, just as for $\theta=0^\circ$. For orbits within the RH islands the electrons make three successive collisions on the RH barrier for each collision with the LH barrier. To interpret the resonant peaks observed in the d^2I/dV^2 versus V plots for

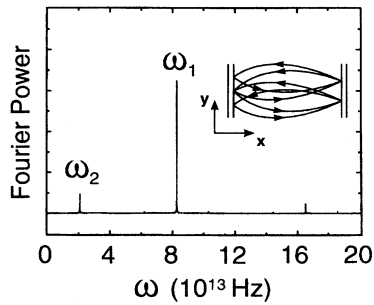


FIG. 5. Fourier power spectrum of $x(t)+z(t)$ (over time t for 5000 traversals of the well) calculated for the stable periodic traversing orbit inset projected on the x - y plane, with $B=10$ T, $\theta=40^\circ$, and $V=1900$ mV.

$V \geq 1.2$ V, we first relate the accessible stable orbits to the corresponding quantized energy levels. Stable orbits should be quantized using the Bohr-Sommerfeld rules rather than the Gutzwiller quantization scheme for chaotic orbits.^{4,8} For each degree of freedom, Bohr-Sommerfeld quantization of stable (though not necessarily periodic) orbits gives rise to well-separated energy levels with nearest-neighbor level spacings $\Delta E_i = \hbar \omega_i$, where $\{\omega_i\}$ are the characteristic frequencies of the motion⁸ for given V , B , and θ . These frequencies can be determined by Fourier transforming any linear combination of the spatial coordinates x, y, z , plotted as a function of time t .⁸ Figure 5 shows the Fourier power spectrum of $x(t)+z(t)$ for the stable traversing orbit inset. This orbit lies within the LH islands of stability in Fig. 4(b) and is periodic. However, similar Fourier spectra are obtained for all stable orbits in this region of phase space irrespective of whether the orbits are periodic or not. The angular frequency of the dominant peak in Fig. 5 is $\omega_1 = 2\pi/\tau$, where τ is the average time between successive collisions on the LH barrier. The separation of the associated energy levels E_j^i , $j=0,1,2, \dots$, is given by $\Delta E^j = \hbar/\tau$. This energy spacing is much larger than the values obtained from the total periods of the *unstable* closed orbits found at lower bias voltages. Consequently, the existence of accessible stable tra-

versing orbits manifests itself in the $I(V)$ plots and derivatives by the appearance of the widely spaced t resonances seen, for example, when $\theta=40^\circ$ and $V > 1.2$ V. A comparison between the voltage spacings calculated for the stable traversing orbits and measured for the t series at $\theta=40^\circ$ is shown in Fig. 3, where we see that the theory overestimates the observed ΔV values. We attribute this to neglect of conduction-band nonparabolicity, which would significantly increase the effective mass of the electron in the potential well since its kinetic energy can reach almost 1 eV. Similar traversing orbits exist at high- V for all values of θ (see right insets to Fig. 2). For these orbits, the time τ between collisions on the LH barrier varies slowly with tilt angle, which accounts for the weak θ dependence of the associated t resonances.

The weaker fundamental peak in the Fourier spectrum shown in Fig. 5 has an angular frequency $\omega_2 \approx \omega_C \cos \theta$ (ω_C is the cyclotron frequency at $B=10$ T) and produces Landau levels $E_2^n = (n + \frac{1}{2})\hbar \omega_C \cos \theta$, $n=0,1,2, \dots$, which are added to the levels E_1^j . This suggests that the motion is at least approximately separable in this region. The Landau-level structure is not observed in tunneling, as for $\theta=0^\circ$, owing to conservation of Landau index n .⁹ Additional weak peaks in the Fourier spectrum occur at frequencies given by linear combinations of ω_1 and ω_2 , but are not related to the energy-level spectrum.

The type-3 stable orbits within the RH set of islands in Fig. 4(b) are not bound by the RH barrier, and so no associated resonances are observed in the tunneling characteristics. However, when AIA barriers are used the electrons cannot surmount the RH barrier and additional resonant features attributable to these orbits are observed in the $I(V)$ plots.⁷

In summary, we have studied the quantized energy levels of a wide 60-nm potential well in a strong tilted magnetic field. For bias voltages and tilt angles within the domain of strong classical chaos, the $I(V)$ characteristics reveal richer structure than for the 120-nm-wide well studied recently,³ because the injected electrons can complete additional unstable periodic orbits before LO phonon emission. The existence of accessible stable orbits for $V \geq 1$ V manifests itself as widely spaced resonances in $I(V)$.

¹C. M. Marcus, A. J. Rimberg, R. M. Westervelt, P. F. Hopkins, and A. C. Gossard, *Phys. Rev. Lett.* **69**, 506 (1992).

²D. Weiss, K. Richter, A. Menschig, R. Bergmann, H. Schweizer, K. von Klitzing, and G. Weimann, *Phys. Rev. Lett.* **70**, 4118 (1993).

³T. M. Fromhold, L. Eaves, F. W. Sheard, M. L. Leadbeater, T. J. Foster, and P. C. Main, *Phys. Rev. Lett.* **72**, 2608 (1994); T. M. Fromhold, L. Eaves, F. W. Sheard, T. J. Foster, M. L. Leadbeater, and P. C. Main, *Physica B* **201**, 367 (1994).

⁴For a review see M. C. Gutzwiller, *Chaos in Classical and Quantum Systems* (Springer-Verlag, New York, 1990).

⁵M. L. Leadbeater, E. S. Alves, L. Eaves, M. Henini, O. H.

Hughes, G. Hill, and M. A. Pate, *J. Phys. Condens. Matter* **1**, 4865 (1989).

⁶T. M. Fromhold, F. W. Sheard, and G. A. Toombs, in *Physics of Semiconductors*, Proceedings of the XX International Conference, edited by E. Anastassakis and J. D. Joannopoulos (World Scientific, Singapore, 1990), p. 1250.

⁷T. M. Fromhold, P. B. Wilkinson, J. Miao, F. W. Sheard, and L. Eaves (unpublished).

⁸N. De Leon and E. J. Heller, *J. Chem. Phys.* **78**, 4005 (1983); M. S. Child, *Semiclassical Mechanics with Molecular Applications* (Oxford University Press, Oxford, 1991).

⁹M. L. Leadbeater, F. W. Sheard, and L. Eaves, *Semicond. Sci. Technol.* **6**, 1021 (1991).